Molecular dynamics study of the ordering of carbon in highly supersaturated α-Fe

C. W. Sinclair,[1] M. Perez,[2] R. G. A. Veiga,[2] and A. Weck[3]
[1]*The Department of Materials Engineering, The University of British Columbia, 309-6350 Stores Road, Vancouver, British Columbia, Canada V6T 1Z4*
[2]*MATEIS, INSA-Lyon, Université de Lyon, UMR CNRS 5510, 69621 Villeurbanne, France*
[3]*The Department of Mechanical Engineering, The University of Ottawa, 161 Louis Pasteur, Ottawa, Ontario, Canada K1N 6N5*
(Received 14 December 2009; published 9 June 2010)

A recently developed Fe-C interatomic potential has been used to investigate carbon in highly supersaturated α iron with an emphasis on the possible ways in which carbon can arrange itself on the octahedral sites of the tetragonally distorted α-iron lattice. Focusing particularly on the composition $Fe_{16}C_2$, the embedded atom method potential used gives the same ground-state structure of $Fe_{16}C_2$ as density-functional-theory calculations. Moreover, when computing C-C interactions between two carbon atoms at 0 K with energy minimization, the preferred separation distance corresponds exactly to the octahedral site positions expected in $Fe_{16}C_2$. It has been shown with molecular dynamics that the carbon atoms in $Fe_{16}C_2$ change how they order on octahedral sites during heating and during cooling. Finally, when investigating the interaction energy of $Fe_{1-x}C_x$ for different carbon compositions, it is found that there is a clear minimum at $x=0.11$ for the fully ordered structure, corresponding to $Fe_{16}C_2$ composition. The results of these calculations are discussed with particular reference to carbon ordering in ferrous martensite.

DOI: 10.1103/PhysRevB.81.224204 PACS number(s): 61.66.Dk, 64.60.Cn, 81.40.Ef

I. INTRODUCTION

The supersaturation of carbon in crystalline α iron is the basis for ferrous martensites and, correspondingly, to an enormous variety of technological applications of significance. One of the particular characteristics of ferrous martensite formed by quenching from high-temperature face centered cubic austenite, is the tetragonality of the martensite lattice. This tetragonality is a direct consequence of carbon ordering onto one of three possible octahedral sites (Fig. 1). An explanation for this ordering was given first in 1948 by Zener[1] who noted that the elastic distortion of the bcc iron lattice could be minimized if the carbon were to reside in only one type of site. This *Zener ordering* model predicts a composition and temperature-dependent transition between ordered and disordered interstitial carbon distributions due to elastic interactions. Khachaturyan[2] has provided a detailed description of the expected strain induced ordering of solutes (both interstitial and substitutional) within the rigorous framework of the so-called "microscopic elasticity theory" (MET). The elastic interaction is, however, only part of the solute interaction in any solid solution system, the other part coming from the chemical interaction. Khachaturyan showed that reliable predictions of the order/disorder transition can only be made if a strongly repulsive chemical interaction is assumed for carbon-carbon interactions. Udyanski *et al.*[3] have recently re-evaluated the calculations of Khachaturyan using a more sophisticated chemical interaction between carbon atoms employing a recently developed embedded atom method (EAM) potential for the Fe-C system and molecular-dynamics simulations. The results of these calculations appear to provide a better correspondence between the order-disorder temperature predicted from MET and experimental observations.

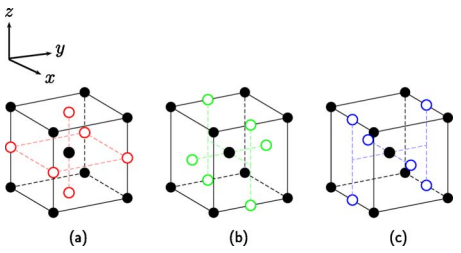

FIG. 1. (Color online) A schematic illustration of the position of octahedral interstitial sites (open circles) in a bcc lattice (filled circles). Here we denote the sites in (a) as z-octahedral sites, those in (b) as y-octahedral sites, and those in (c) as x-octahedral sites due to their alignment along these respective axes.

The above-described theories of carbon ordering have been applied to carbon supersaturations typical of ferrous martensites, e.g., <1 wt % C (<4.48 at.% C) but not to higher levels of supersaturation.[4] There are, however, numerous examples where much larger supersaturations can be achieved. Very large supersaturations can be obtained from phase transformation as in the crystallization of amorphous Fe-C (Ref. 5) and direct synthesis by vapor deposition, e.g., Ref. 6. Similar levels of supersaturation can be achieved through severe plastic straining, as in the case of the decomposition of cementite during wire drawing[7,8] and in rail steels that form white etching layers (e.g., Ref. 9).

In martensite as well, it is possible to achieve locally high supersaturations of carbon during the very early stages of tempering (see, e.g., Ref. 10 for a review). A ferrous martensite quenched from austenite without tempering (i.e., no reordering of carbon during cooling), if held at temperatures close to room temperature will decompose to form a modulated structure comprised of carbon-rich and carbon-lean areas.[10] Early work by TEM (e.g., Ref. 11) and Mössbauer spectroscopy (e.g., Ref. 12) identified the carbon-rich regions as substoichiometric γ'-Fe_4C (see, e.g., Ref. 13) in supersaturated ferrite. More recent TEM and one-dimensional atom probe tomography in the 1980s provided evidence that the modulated structure is the product of spinodal

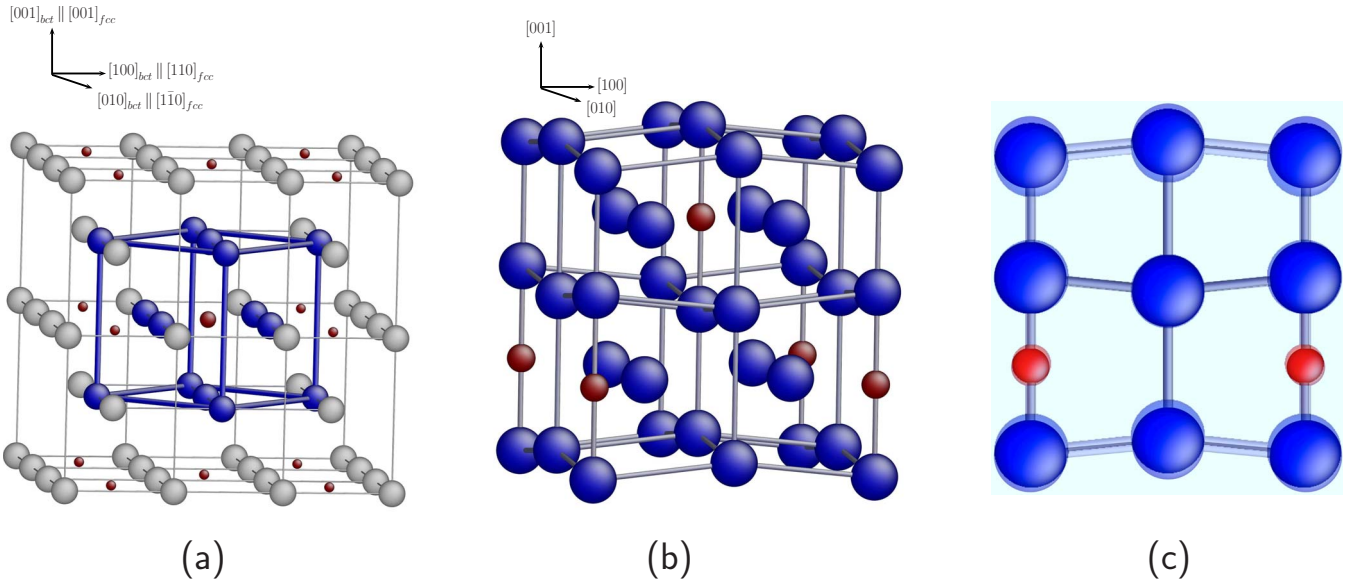

FIG. 2. (Color online) (a) The γ'-Fe_4C carbide illustrating the position of carbon atoms (small spheres) situated in z-octahedral sites of the body-centered tetragonal lattice. This can also be described as carbon in the octahedral sites of a face centered cubic iron lattice, an fcc unit cell being highlighted by the dark (blue) atoms. The position of atoms in this image have been determined by molecular statics at zero pressure using the EAM potential described in section Ia. (b) The α''-$Fe_{16}C_2$ carbide illustrating the position of carbon atoms (small spheres) situated in z-octahedral sites of the body-centered tetragonal lattice. This structure is formed by the systematic removal of half of the carbon atoms from the γ'-Fe_4C structure in (a). As with the γ' structure shown in (a), the α'' unit cell shown in (b) was obtained by molecular statics at zero pressure. (c) To show the similarity of the atomic positions predicted from MD and DFT, the {100} plane of the α''-$Fe_{16}C_2$ carbide is plotted with the atomic positions in this plane being superimposed from the two calculation schemes.

decomposition.[4,10] As noted above, rather than being stoichiometric Fe_4C, the carbon-rich regions tended to have a carbon content closer to 10 at. %,[14] a point that was highlighted by Ino *et al.*[15] who denoted it as Fe_4C_x with $x \ll 1$. Taylor *et al.*[4] on the basis of their original TEM and atom probe data on Fe-Ni-C martensites along with previous work including Mössbauer spectroscopy proposed that instead of γ'-Fe_4C, the carbon-rich regions could be better described as α''-$Fe_{16}C_2$, which is isostructural to the metastable α''-$Fe_{16}N_2$ nitride.[16,17] The α''-$Fe_{16}C_2$ differs from the γ'-Fe_4C structure only in that one half of the carbon atoms are systematically removed in the former relative to the latter (Fig. 2).[4] With the advent of more powerful electron microscopy and three-dimensional tomographic atom probe, there has been an attempt to revisit this question. Some recent results appear to support the results of Taylor *et al.* (e.g., Ref. 18) while other results have led to questions about the structure, stability, and conditions required for the formation of $Fe_{16}C_2$ (e.g., Refs. 19 and 20).

Both the γ'-Fe_4C and α''-$Fe_{16}C_2$ can be described as being comprised of carbon situated in an ordered configuration on the octahedral sites of a tetragonally distored body centered cubic α-Fe lattice. While it is well known that in dilute systems, characterized at low temperature, carbon tends to organize onto one of the three types of octahedral sites in Fig. 1, at high supersaturations consideration of further ordering on this type of octahedral site might be important. Thus one can consider at least three conditions: (1) carbon disordered on all octahedral sites, (2) carbon ordered onto one octahedral site but not spatially organized on this octahedral site (partially ordered), and (3) carbon ordered onto one octahedral site with occupation of only some of these sites leading to a fully ordered structure.

For compositions close to 11 at. % C and for "low" temperatures, Taylor *et al.* argued that the lowest free energy among these three choices may correspond to the fully ordered α''-$Fe_{16}C_2$ structure. The partially ordered structure (denoted here as α'-Fe_8C, following the literature for the Fe-N system) would be the next most stable while the least stable would correspond to carbon distributed equally among the three octahedral sites (denoted here as α-Fe-C). For lower carbon contents, a similar situation may occur with nonstoichiometric α'', where the free energy of α'' and α' will converge in the limit of dilution. Between the three cases described above a continuous sequence of ordered structures may exist connecting the α'' and α' structures. Experimental evidence that ordering beyond the Zener Ordered α' structure may exist even in untempered ferrous martensites comes from the observation, based on Mössbauer spectroscopy, that the carbon-carbon nearest-neighbor distance is similar to that expected within the α''-$Fe_{16}C_2$ structure.[12]

In this work we have sought to examine the various possible ways that carbon can order itself on octahedral sites within the α-iron lattice with specific focus on the composition corresponding to α''-$Fe_{16}C_2$. To do this, molecular statics and molecular dynamics (MD) have been applied using a recently developed interatomic potential for the Fe-C system specifically fit based on the interaction energy between carbon interstitials and lattice defects. The goal here is restricted to illustrating the relative thermal stability of interstitial carbon ordering in iron, the iron atoms being on a body-

TABLE I. Ground-state ($T=0$ K) total energy and lattice parameters of the various Fe-C structures as computed from the EAM potential. Also shown for reference are the lattice parameters predicted from DFT calculations on the $Fe_{16}C_2$ structure. The α'-Fe_8C has been derived by cooling from 1700 to 900 K and holding for 10 ns followed by quenching to 0 K.

Property	α''-$Fe_{16}C_2$ (EAM)	α''-$Fe_{16}C_2$ (DFT)	α'-Fe_8C (Zener ordered)	α-$FeC_{0.111}$
Energy, eV/atom	−4.704		−4.692	−4.673
Lattice parameter, a (Å)	5.6803	5.71	5.678	5.804
Lattice parameter, c (Å)	6.072	6.31	6.088	5.844
Tetragonality, c/a	1.069	1.105	1.072	1.007

centered tetragonal lattice. A more detailed examination of the thermodynamics of this system will be described in a future communication.

II. SIMULATION PROCEDURES

A. Fe-C EAM potential

The 2007 Raulot-Becquart Fe-C EAM potential[21] has been used in this work. In this potential the Fe-Fe interactions have been taken from the work of Mendelev *et al.*[22] while the Fe-C portion was obtained from fitting to density-functional-theory (DFT) calculations aimed at capturing the interaction between two carbon atoms, carbon atoms on different interstitial sites, and interaction between carbon atoms and defects (e.g., vacancies) in the bcc-Fe lattice. The potential has been shown to replicate well the tetragonality of the bcc-iron lattice with increasing carbon content as well as the activation energy for diffusion.[21] It has also been recently used to examine the interaction between carbon and dislocations in bcc-iron.[23] Despite recent advances, it is well recognized that there are certain aspects of the Fe-C system that are impossible to capture with a classical EAM potential. In the case of iron, the lack of a magnetic contribution to the energy of the system has several consequences including the over stabilization of the bcc structure, leading to the free energy of the fcc structure being higher than the bcc structure at all temperatures.[24] Thus, in the calculations presented here it is possible to study the transitions of bcc-Fe to the melting point without the formation of the fcc-austenite phase. Another particular aspect of EAM Fe-C potentials is their inability to describe the directionality of the bonding in covalently bonded materials. Thus, the Raulot-Becquart potential does not attempt to capture the high carbon end of the phase diagram. While these are important issues, we believe that the potential used captures the physics of the most important aspects of the processes studied here correctly as will be discussed below.

B. Density-functional calculations

As a reference for the simulations with the EAM potentials, spin-polarized *ab initio* calculations were performed with the SIESTA code,[25] which uses a localized linear combination of atomic orbitals as basis set in order to solve the Kohm-Sham equations. The generalized gradient approximation with the exchange correlation functional of Perdew, Burke, and Ernzerhof[26] was employed in these calculations. The charge density was projected onto a real-space grid with an equivalent cutoff of 350 Ry. Sampling of the Brillouin zone was performed by a $6\times6\times6$ grid according to the Monkhorst-Pack scheme. Iron and carbon atomic cores were represented by norm-conserving Trouiller-Martins pseudopotentials.[27] A single $Fe_{16}C_2$ unit cell and periodic boundary conditions were used in the calculations. Conjugate gradient was applied to minimize the system total energy, optimizing atomic coordinates, and also the cell lattice parameters with a zero pressure target. The results are summarized in Table I.

C. Building the $Fe_{16}C_2$ structure

Fully periodic simulation boxes were constructed from $10\times10\times10$ bcc-iron unit cells. Carbon was inserted into the octahedral sites consistent with their positions in the α''-$Fe_{16}C_2$ structure. This cell, containing 2000 Fe atoms and 250 carbon atoms, was subsequently subjected to molecular statics employing conjugate gradient minimization under the constraint of constant volume. The molecular statics calculations were iterated, modifying the box size after each iteration so as to reduce the stresses acting in the x, y, and z directions to less than 100 MPa. One unit cell of the ground state α'' structure obtained after this procedure is illustrated in Fig. 2(b).

Studies on the thermal stability of the Fe-C system were performed using both ramped and isothermal molecular-dynamics simulations. In these cases the simulations were performed in an isothermal-isobaric (NPT) ensemble with the pressure targeted to be zero along all directions of the simulation cell. The temperature and pressure in these simulations were controlled using a Nosé-Hoover thermostat. All of the above simulations have been performed using LAMMPS (www.lammps.sandia.gov).[28]

D. Analysis tools

In order to interpret the results obtained from these simulations, particularly in reference to the ordering of carbon atoms, two tools have been used. First the pair correlation function between carbon atoms has been computed periodically for all simulations. This is sensitive to the degree of ordering of carbon atoms on octahedral sites and can be used, in particular, to help to distinguish between the α'' and α' structures where carbon in both cases sits on one type of

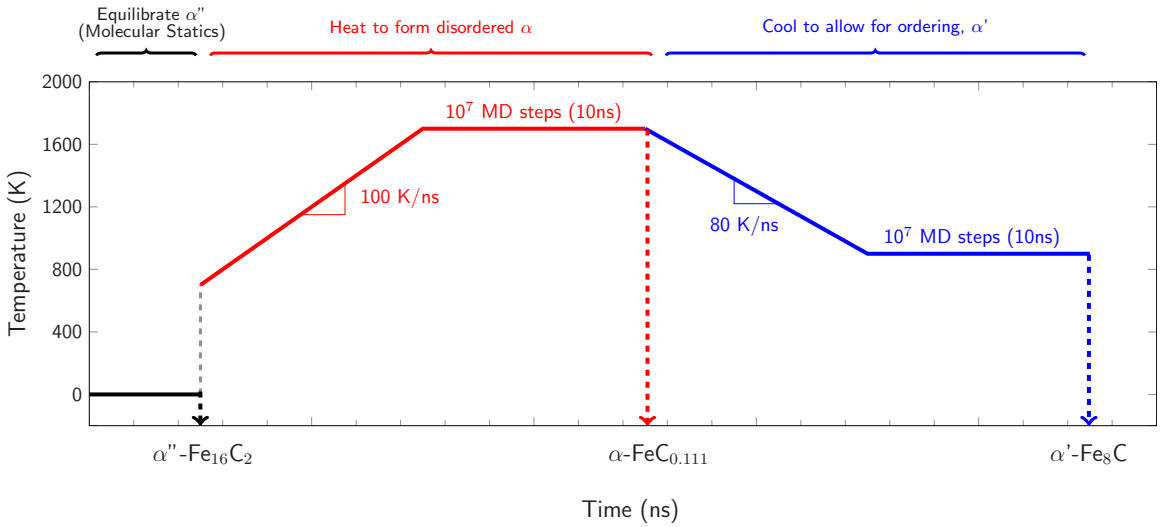

FIG. 3. (Color online) A schematic illustration of the thermal profile imposed starting from the ideal α''-$Fe_{16}C_2$ ordered phase in order to produce the α'-Fe_8C and α-Fe-C phases.

octahedral site. The fraction occupation of the three types of octahedral sites in Fig. 1 is computed by considering the nearest-neighbor iron atom to each carbon atom. For carbon situated in the z sites shown in Fig. 1 the nearest-neighbor iron atom is located along the z axis of the simulation cell. Similarly in the case of x and y octahedral sites the nearest-neighbor iron is located along the x and y directions, respectively. In this way one can readily distinguish between the α structure where carbon atoms are situated on all three types of octahedral sites and the α'' and α' structures were carbon orders onto only one octahedral site.

III. EXPLORATION OF Fe-C ORDERING STARTING FROM α''-$Fe_{16}C_2$

The starting point for our exploration of the ordering of carbon in the Fe-C system is the α''-$Fe_{16}C_2$ structure equilibrated at $T=0$ K using molecular statics as described above. Table I gives some of the ground-state characteristics of this structure (tetragonality, ground-state energy, and interaction energy) based on the EAM potential used. It is noteworthy that, at 0 K the α''-$Fe_{16}C_2$ phase has the lowest energy and thus would be predicted to be most stable. Also shown in this table are the same parameters calculated using density-functional theory. As can be seen, the ground-state structures predicted based on the EAM potential and the DFT calculations are very similar [Fig. 2(c)]. These results provide some confidence that the EAM potential used in this work is able to capture the basic aspects of this problem even at these nondilute carbon concentrations.

In order to explore the thermal stability and other possible carbon distributions in this system, a series of molecular-dynamics simulations were performed. Figure 3 illustrates the thermal cycle applied to the simulation cell.

The equilibrated α'' structure was heated at a constant rate of 100 K/ns from 700 to 1700 K in 10^7 time steps (10 ns). Heating was started from 700 K since, based on the carbon diffusivity predicted by this potential,[21] the probability of carbon jumps is negligible below 750 K for the time scales considered here. Above ~1500 K the α'' structure is unstable and converts to the disordered α structure with equal occupancy of x, y, and z octahedral sites. This is reflected in the absence of tetragonality of the simulation box at temperatures above ~1600 K (Fig. 4). The pair correlation function (Fig. 5) also indicates the presence of the disordered α structure at 1700 K. Here the "ideal" positions of peaks in the pair correlation function have been calculated assuming random occupation of *all* octahedral sites (open circles) and for random occupation of *one* octahedral site (solid circles). One can see that the peak at approximately $r=0.35$ nm is characteristic of the disordered α structure.

One interesting point to note is that even in the apparently disordered α phase formed at high temperature, not all octahedral sites are occupied. In Fig. 5 one observes that there is no density corresponding to the two nearest-neighbor positions (at approximately 1.5 and 2 Å). This is consistent with all observations we have made on the α phase where carbon nearest neighbors are never observed. This impacts on the goodness of fit between the ideal pair correlation peak positions in Fig. 5(b) and the computed function owing to the fact that the local strains induced by the nonrandom interstitial occupation locally distorts the lattice. The result is well evidenced by the poor fit between the peak at approximately $r=0.35$ nm and the corresponding ideal position.

In order to explore the possible conversion of the "disordered" α structure obtained at 1700 K to the original α''-$Fe_{16}C_2$ structure from which we started, we have taken the structure, after holding for 10 ns at 1700 K, and cooled it at a rate of 80 K/ns to 900 K. The simulation was then held isothermally for a further 10 ns at this temperature. The box shape evolution with cooling is shown in Fig. 4. As noted above, below 750 K we do not expect structural transitions within the simulation times considered here since the kinetics of carbon (and iron) diffusion are too slow. However, at 900 K there is sufficient thermal activation for carbon to make several atomic jumps within the 10 ns holding time.

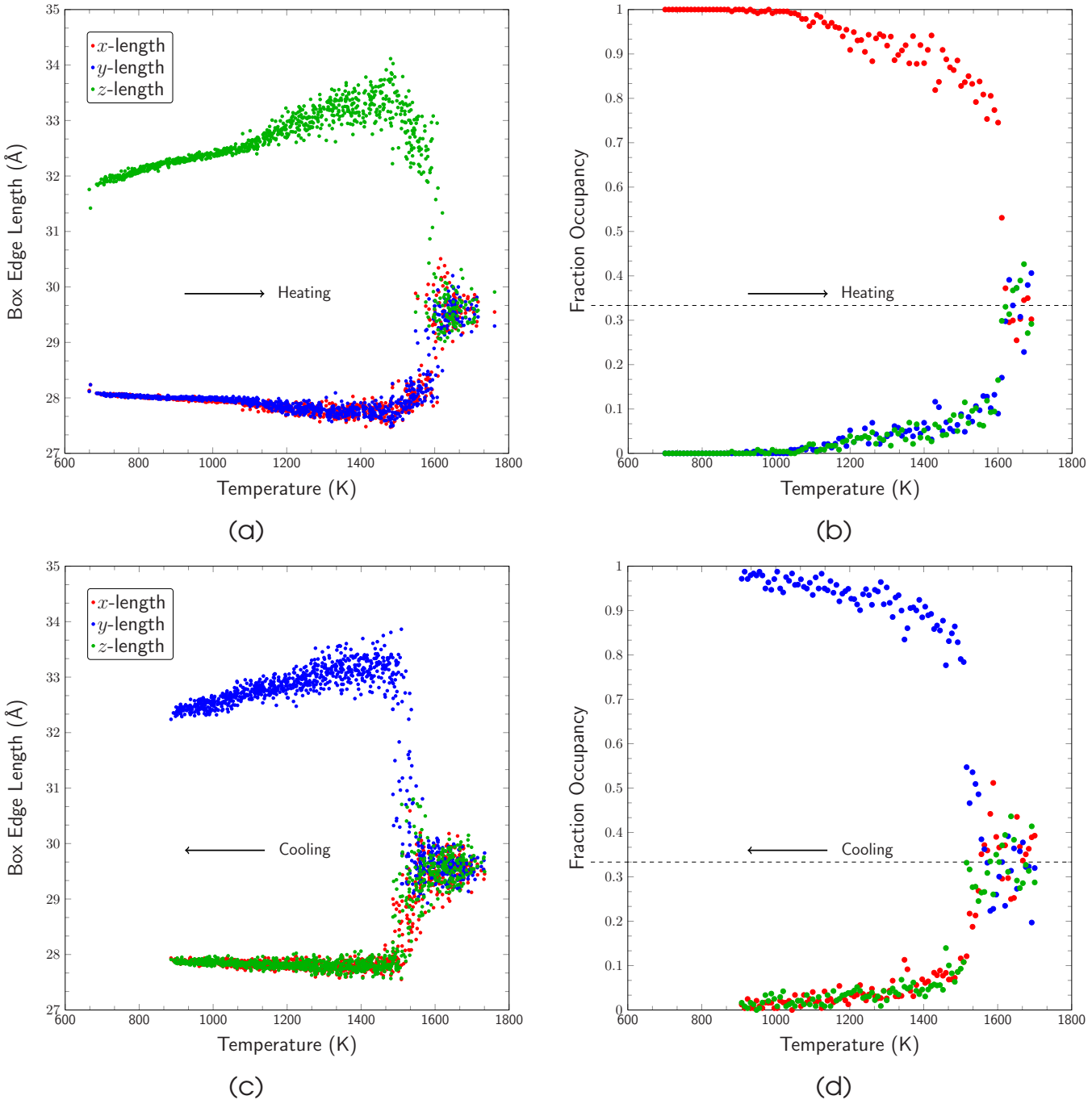

FIG. 4. (Color online) The box size and fraction occupation of the x-, y-, and z-type octahedral sites during [(a) and (b)] heating from 700 to 1700 K and [(c) and (d)] during cooling from 1700 to 900 K. The plots show similar trends owing to the fact that as carbon orders onto one type of octahedral site the tetragonality of the lattice increases.

In Fig. 4 we observe the re-emergence of tetragonality of the lattice as we cool below ~1600 K. This is reflected in a change in the fraction occupation of the octahedral sites from equal occupation to occupation of only one site. However, this information is not sufficient to distinguish between the α'' and α' structures since each is expected to have carbon residing on only one type of the x, y, or z octahedral sites. In this case the pair correlation function (Fig. 5) illustrates that the structure formed at 900 K is different from the starting α'' structure and has peaks characteristic of the carbon-carbon spacing expected in the α' structure. Again, however, it is noteworthy that the closest possible carbon-carbon distance does not appear in the structure.

The results in Fig. 4 illustrate the change in ordering of carbon observed on heating and cooling. These transformations can also be witnessed if the volume of the simulation box is plotted as a function of temperature (Fig. 6). From Fig. 6 we can also more precisely define the temperatures at which the transformations between α'', α', and α occur. In particular, four temperatures are highlighted in Fig. 6. Owing

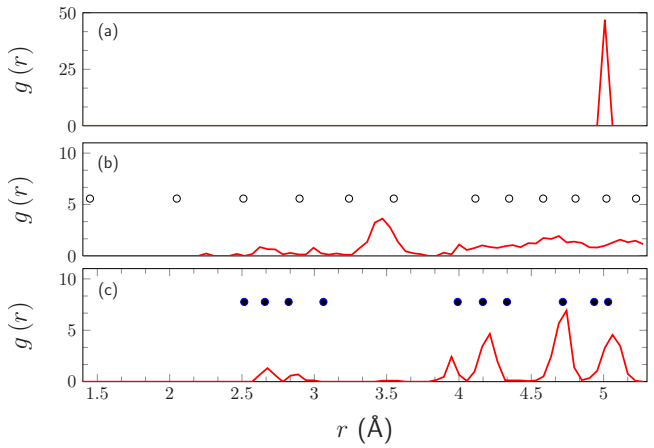

FIG. 5. (Color online) (a) The pair correlation function at 0 K for the starting α''-$Fe_{16}C_2$ structure. (b) The pair correlation function for the system after holding at 1700 K for 10 ns, followed by quenching to $T=0$ K. (c) The pair correlation function based on the structure formed by holding at 1700 K followed by cooling to 900 K, holding for 10 ns, and finally quenching to $T=0$ K. Idealized theoretical carbon-carbon interatomic distances for carbon residing in octahedral sites are shown as circles above the curves in figures (b) and (c). The open circles represent the peak positions associated with carbon randomly occupying all octahedral sites while the solid circles represent peak positions when carbon resides randomly in only one of these octahedral sites.

to the high heating and cooling rates employed in these simulations, it is impossible to comment on the true *equilibrium* temperatures for the transformations as the kinetics of carbon diffusion limits the rate at which these transformations can be completed. This is particularly exacerbated at low temperatures where no evidence of the transformation from $\alpha' \rightarrow \alpha''$ is observed on cooling. We have, however, performed long time (up to 0.1 μs) NPT simulations at 800 °C (zero pressure) and have observed that α''-$Fe_{16}C_2$ slowly decomposes toward α'. This implies that the equilibrium transformation temperature between α'' and α' is below 800 °C and therefore inaccessible within reasonable simulation times. On the other hand, the transformation between α' and α'' can be clearly observed to occur within a relatively narrow temperature range in Fig. 6. While it is not possible to comment definitively on the nature of this transformation due to the kinetic factors noted above, it would appear that the transformation is first order based on the change in volume between 1475 and 1525 °C. The hysteresis between the behavior at high temperature on heating and cooling is also attributable to kinetic effects. Indeed, upon cooling from a fully disordered α structure the carbon must reorder, a process that requires each carbon atom to make several atomic jumps. The process of disordering from α', on the other hand, could be accomplished simply by each carbon atom making a single atomic jump. This point, as well as the nature of the transformations between α''/α' and α''/α' require further exploration. This work is currently underway.

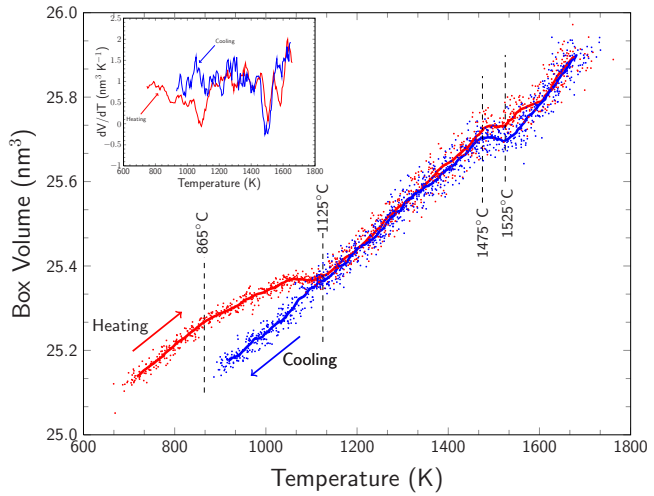

FIG. 6. (Color online) Simulation box volume as a function of temperature during heating and cooling. The solid lines are a moving average of the data, illustrating the average trends in volume change. Inset, the thermal expansion of the box based on the smoothed data is plotted as a function of temperature.

IV. RATIONALIZING THE ABOVE OBSERVATIONS BASED ON STRAIN-INDUCED CARBON ORDERING

In the observations described above, one can clearly observe three distinct structures corresponding to three different ways of organizing carbon on octahedral sites in tetragonally distorted bcc Fe. Cooling from high temperature, there is a transition from the disordered high-temperature α phase where all three octahedral sites in Fig. 1 can be occupied, to a structure where only one of these three octahedral sites can be occupied consistent with the common concept of the Zener ordered α' phase. It is noteworthy, however, that the occupation of allowed octahedral sites in both these cases is not random. In particular, carbon atoms tend to avoid nearest- (and possibly second nearest) neighbor configurations. Further cooling, however, does not allow one to observe the transition from the α' phase to the α'' phase due to kinetic limitations. The α'' phase is the phase with the lowest ground-state energy (among these three) when compared after quenching from 1700 and 900 K, respectively, as seen in Table I.

As noted above, the artificial stability of bcc Fe versus fcc Fe at high temperature introduced by the EAM potential used allows us to study the hypothetical α' to α transition occurring at high temperature. While this transition is of interest from a theoretical point of view, it is the α'' to α' transition that is of practical interest due to its relation to the ordering of carbon in ferrous martensite discussed above. In order to examine more closely the strain-induced interaction between carbon atoms in the α' and α'' structures we have performed two simple simulations. A large simulation box consisting of 16 000 iron atoms was generated at $T=0$ K. Two carbon atoms were next placed on octahedral sites within this box. The position of one carbon atom was fixed, to reside within a z-octahedral site while the second was moved to other octahedral sites. For all configurations of the two atoms, energy minimization employing a conjugate gradient method was used to find the energy of the system as a function of the separation distance between the carbon atoms.

The energies obtained in the above calculations contain a contribution to the total energy arising from both chemical interactions as well as the interaction between one carbon atom and the elastic strain field resulting from the other. In order to separate these two contributions to the ground-state energy, a second calculation was made. After minimization of the energy of the Fe-C simulation box containing two carbon atoms, the carbon atoms were deleted leaving the Fe lattice elastically distorted. The energy of this distorted iron lattice was then calculated giving a simple measure of the elastic strain energy induced by the carbon atoms without the chemical contribution arising from Fe-C and C-C interactions. These results have consequences for the interpretation of the properties and stability of, for example, ferrous martensites subjected to low-temperature tempering.

In order to be able to quantitatively compare these results, we have computed an interaction energy between carbon atoms based on these simulations. The interaction energy per carbon atom (ΔE_{inter}) has been defined as

$$\Delta E_{inter} = \frac{1}{N_C}[(E_{total} - E_{Fe}) - N_C(E_{1C} - E_{Fe})], \qquad (1)$$

where E_{total} is the total energy of the simulated system containing N_C carbon atoms for the above simulations. The energy E_{Fe} is the energy of N_{Fe} iron atoms. The energy E_{1C} is the energy of a simulation cell consisting of one carbon atom within a bcc lattice consisting of N_{Fe} iron atoms. Physically, the first term in Eq. (1) is the energy associated with the carbon atoms in a system containing N_C interacting carbon atoms while the second term is the energy associated with a system of the same size containing noninteracting carbon atoms. A negative value of ΔE_{inter} implies that the interaction between carbon atoms tends to lower the energy of the system relative to a system containing noninteracting carbon atoms and thus should be preferred.

Figure 7 illustrates the results of these calculations taking the first (fixed) carbon atom as residing in a z-octahedral site. The results have been separated to examine the interaction of carbon atoms along particular directions relevant to the directions between carbon atoms expected in the α'' structure. In Fig. 7(a) the second carbon atom is moved along the $[001]_{Fe}$ direction, in Fig. 7(b) it has been moved along the $[111]_{Fe}$ direction and in (c) it has been moved along the $[100]_{Fe}$ direction.

As expected, with increasing separation distance between the two carbon atoms, $\Delta E_{inter} \rightarrow 0$ corresponding to the condition where no interaction takes place. However, at short distances one can see significant variations in ΔE_{inter} as a function of carbon-carbon spacing.

More importantly, the above results show that beyond the second nearest-neighbor distance, the elastic strain energy (open symbols) alone is able capture the interaction energy properly. At closer distances the elastic strain energy and the total strain energy diverge with the chemical interaction between carbon atoms causing the interaction energy to become large and positive (repulsive interaction) while the elastic interaction alone prefers, at short distances, that the carbon atoms sit on top of one another. The results shown in Fig. 7 are separated to show spacings along certain directions

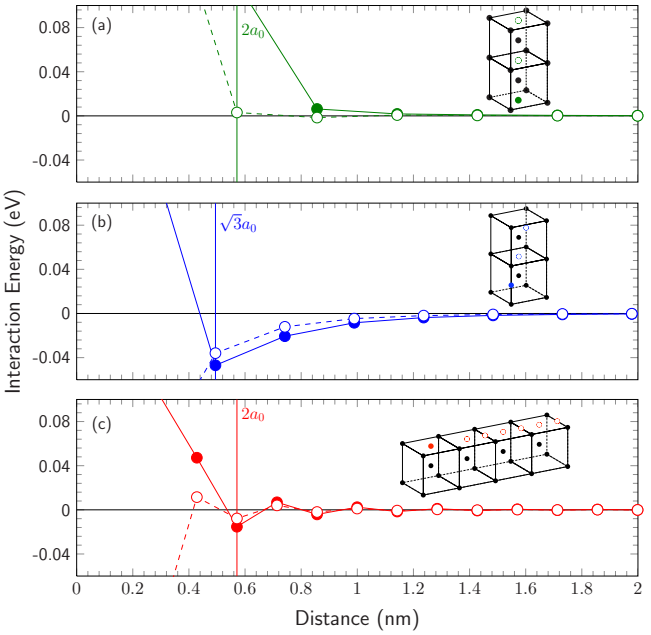

FIG. 7. (Color online) The interaction energy at $T=0$ K between two carbon atoms as a function of their separation distance. The first carbon atom was placed within a z-octahedral site and the second carbon atom moved along the (a) $[001]_{Fe}$ direction, (b) $[111]_{Fe}$ direction, and (c) $[100]_{Fe}$ direction. The filled symbols represent the energy calculations with chemical interactions considered while the open symbols represent the energy when only the elastic distortion caused by the carbon atoms are considered. One can observe minima in (b) and (c) corresponding to preferred sites with separation distances of $\sqrt{3}a$ and $2a$. These correspond to octahedral site positions expected in α''-$Fe_{16}C_2$. Note that the interaction energy here is the total interaction energy and not the interaction energy per carbon atom as in Eq. (1). Thus the interaction energy here is $\Delta E_{inter} N_C$, where $N_C=2$.

in the iron lattice so as to make the link to the α'' structure clearer. One important observation from these calculations is that the first minima in the interaction energy along the $[100]_{Fe}$ and $[111]_{Fe}$ directions corresponds to the separation between the occupied octahedral sites in the α'' structure. There is no energy minima along the $[001]_{Fe}$ direction as predicted from density-functional-theory calculations.[21]

The very strong rise in interaction energy at close distances between carbon atoms helps to explain why the first and second nearest-neighbor positions and the first nearest-neighbor distances in the α and α' structures, respectively, are not observed at $T=0$ K. With increasing temperature entropic effects can come to dominate explaining the progressive transformation from the most highly ordered structure (α'') to the α' and finally α structures with increasing temperature.

V. COMPOSITION DEPENDENCE OF THE STABILITY OF ORDERING

While so far this work has focused on the fixed composition corresponding to the stoichiometric α''-$Fe_{16}C_2$, we briefly touch here on the hypothesis made by Taylor *et al.*[4]

that the form of ordering observed in α'' may be actually provide the lowest-energy structure over a range of compositions. The results shown above for the interaction energy between two carbon atoms would suggest that even in the dilute limit there are specific octahedral positions which carbon atoms would prefer to reside in and that these positions correspond to the positions of the carbon atoms in the α'' phase.

To explore this possibility a series of simulations were performed on samples having compositions ranging from 0 at. % carbon to 12 at. % carbon. In each case a simulation similar to those described above was performed. For substoichiometric compositions, carbon was randomly removed from the stoichiometric α'' followed by relaxation to zero pressure and minimum energy via molecular statics. This structure was next heated at 100 K/ns to 1700 K and held for 10 ns. The resulting α structure was subsequently quenched to $T=0$ K, the energy and pressure being minimized by molecular statics. Also, the α structure formed at 1700 K was cooled to 900 K and held to form α'. This was followed by quenching to $T=0$ K and energy minimized by molecular statics adjusting to also have zero pressure. As an alternative method to form α', the starting substoichiometric α'' was heated at 100 K/ns to 900 K directly and held for 10 ns. This was then quenched to $T=0$ K, energy minimized and relaxed to zero pressure. For superstoichiometric compositions the same procedure was followed but the starting structure was produced by starting from the stoichiometric α'' structure, adding extra carbon to octahedral sites consistent with the γ'' structure (cf. Fig. 2).

The results in Fig. 8 show several interesting characteristics. First, one notes that the α''-like ordering of interstitials results in the most preferable interstitial interaction over the full range of compositions studied, whereas the disordered α always shows unfavorable interactions. This shows remarkable agreement with the qualitative ideas suggested by Taylor *et al.*[4] (cf. Fig. 20 of Ref. 4). One can see, as well, that at high carbon contents close to the stoichiometric α'' composition, the energy (and structures) predicted for the α' formed by heating and cooling are not the same. This is likely a consequence of the fact that atomic mobility is too slow at this temperature for the structure to have found its minimum energy configuration. One also notes that there are no measurements for the α' at compositions less than 8 at. % C. This arises from the fact that at lower carbon contents the stable structure at 900 K is actually α and not α'. Thus, in order to obtain the α' structure it is necessary to go to lower temperatures and longer simulation times. Finally, for compositions above the stoichiometric α'' composition we found that upon heating to 1700 K the α phase was not formed. Instead, at a temperature close to 1400 K the structure converted to the fcc-austenite phase, which one could consider to be a substoichiometric γ' carbide.

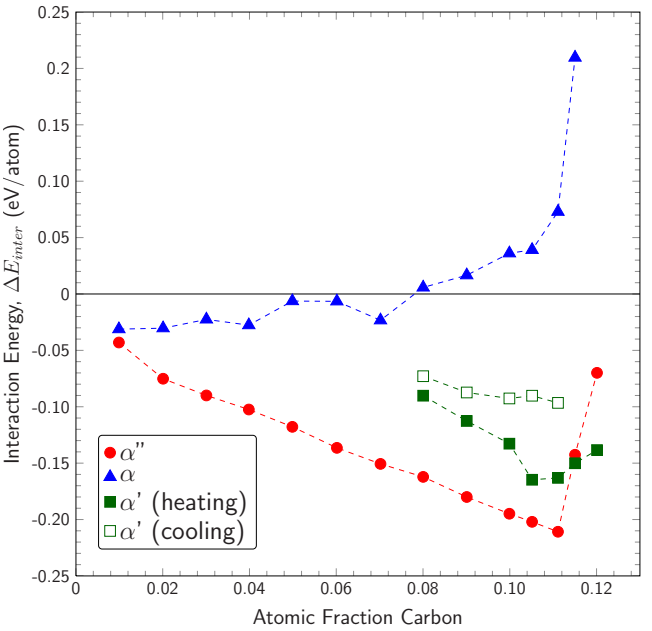

FIG. 8. (Color online) The interaction energy between carbon atoms for α'', α', and α structures as a function of composition. The α' structures have been formed either by cooling from the high-temperature α phase at 1700 to 900 K or by heating α'' from $T=0$ to 900 K.

VI. SUMMARY

The results of these simulations provide valuable information on the ordering of interstitial carbon in bcc-iron. The observation of α''-$Fe_{16}C_2$ having the most favorable carbon-carbon interactions is consistent with the concepts proposed by Taylor *et al.*[4] in the spinodal decomposition of martensite. It is also, however, consistent with experimental studies at much lower carbon contents where it is found that the carbon-carbon neighbor spacings are those consistent with an α''-like ordering. While, we do not consider the formation of other carbides in these simulations, the results do suggest the possibility for forming α''-$Fe_{16}C_2$ if sufficiently far from equilibrium conditions can be obtained. Moreover, the results represent a starting point for revisiting the low-temperature phase equilibria in the Fe-C system.

ACKNOWLEDGMENTS

The authors would like to thank Colin Scott, ArcelorMittal Global Research Centre, Maiziéres-les-Metz France for his comments on this work.

[1] C. Zener, Phys. Rev. **74**, 639 (1948).
[2] A. G. Khachaturyan, *Theory of Structural Transformations in Solids* (Wiley, New York, 1983).
[3] A. Udyansky, J. von Pezold, V. N. Bugaev, M. Friák, and J. Neugebauer, Phys. Rev. B **79**, 224112 (2009).
[4] K. A. Taylor, L. Chang, G. B. Olson, G. D. W. Smith, M. Cohen, and J. B. V. Sande, Metall. Trans. **20A**, 2717 (1989).
[5] E. Bauer-Grosse, Thin Solid Films **447-448**, 311 (2004).
[6] S. D. Dahlgren and M. D. Merz, Metall. Trans. **2**, 1753 (1971).
[7] V. N. Gridnev and V. G. Gavrilyuk, Phys. Met. **4**, 531 (1982).
[8] J. Languillaume, G. Kapelski, and B. Baudelet, Acta Mater. **45**, 1201 (1997).
[9] W. Lojkowski, M. D. Jahanbakhsh, G. Bürkle, S. Gierlotka, W. Zielinski, and H. J. Fecht, Mater. Sci. Eng. **303**, 197 (2001).
[10] G. B. Olson and W. S. Owen, *Martensite. A Tribute to Morris Cohen* (ASM International, Metals Park, Ohio, 1992).
[11] V. I. Izotov and L. M. Utevskiy, Phys. Met. Metall. USSR **25**, 86 (1968).
[12] W. K. Choo and R. Kaplow, Acta Metall. **21**, 725 (1973).
[13] G. B. Olson and M. Cohen, Metall. Trans. **14A**, 1057 (1983).
[14] M. K. Miller, P. A. Beaven, S. S. Brenner, and G. D. W. Smith, Metall. Trans. **14A**, 1021 (1983).
[15] H. Ino, T. Ito, S. Nasu, and U. Gonser, Acta Metall. **30**, 9 (1982).
[16] K. H. Jack, Proc. R. Soc. London **208**, 200 (1951).
[17] K. H. Jack, J. Alloys Compd. **222**, 160 (1995).
[18] C. Zhu, A. Cerezo, and G. D. W. Smith, Ultramicroscopy **109**, 545 (2009).
[19] J.-M. R. Génin, Metall. Trans. **21**, 2083 (1990).
[20] M. J. Van Genderen, M. Isac, A. Böttger, and E. J. Mittemeijer, Metall. Mater. Trans. **28A**, 545 (1997).
[21] C. S. Becquart, J. M. Raulot, G. Bencteux, C. Domain, M. Perez, S. Garruchet, and H. Nguyen, Comput. Mater. Sci. **40**, 119 (2007).
[22] M. I. Mendelev, S. Han, D. J. Srolovitz, G. J. Ackland, D. Y. Sun, and M. Asta, Philos. Mag. **83**, 3977 (2003).
[23] E. Clouet, S. Garruchet, H. Nguyen, M. Perez, and C. S. Becquart, Acta Mater. **56**, 3450 (2008).
[24] C. Engin, L. Sandoval, and H. M. Urbassek, Modell. Simul. Mater. Sci. Eng. **16**, 035005 (2008).
[25] J. M. Soler, J. D. Gale, J. J. A. García, P. Ordejón, and D. Sanchéz-Portal, J. Phys.: Condens. Matter **14**, 2745 (2002).
[26] J. P. Perdew, K. Burke, and M. Ernzerhof, Phys. Rev. Lett. **77**, 3865 (1996).
[27] N. Troullier and J. L. Martins, Phys. Rev. B **43**, 1993 (1991).
[28] S. J. Plimpton, J. Comp. Phys. **117**, 1 (1995).